International Journal of Engineering and Technology Innovation, vol. 8, no. 2, 2018, pp. 118-132

Applicability of Various Load Test Interpretation Criteria in Measuring Driven Precast Concrete Pile Uplift Capacity

Maria Cecilia M. Marcos[1], Yit Jin Chen [2, *]

[1]Department of Civil Engineering, Adamson University, Manila, Philippines.

[2]Department of Civil Engineering, Chung Yuan Christian University, Chung-Li, 32023, Taiwan.

Received 25 July 2017; received in revised form01 October 2017; accepted 10 October 2017

Abstract

This paper presented a comprehensive analysis of load test interpretation criteria to determine their suitability to driven precast concrete (PC) pile uplift capacity. A database was developed containing static pile load tests and utilized for the evaluation. The piles were round and square cross-sections under drained and undrained loading. To explore and compare their behavior, the stored data were categorized into four groups. In general, the trends of every criterion for the four groups were notably the same. In both drained and undrained loading, slightly larger interpreted capacities were demonstrated by square piles than by round piles. Moreover, round piles demonstrated more ductile load-displacement response than square piles especially in undrained loading. Statistical analyses presented that smaller values of displacements exhibited higher coefficient of variation. The drained and undrained tests were compared and results showed less variability in drained than undrained loading and capacity ratios (Qx/QCHIN) in drained loading were slightly higher than in undrained loading. The interrelationship and applicability of these criteria as well as the design recommendations in terms of normalized capacity and displacement were given based on the analyses.

Keywords: driven precast concrete piles, uplift, interpretation criteria, database

1. Introduction

Reinforced concrete has been widely used for building construction either as a part of building or whole structure [1]. As a foundation, driven precast concrete (PC) piles are common for high rise buildings, bridges and towers. When driven precast concrete (PC) piles are used as a foundation for bridges, towers, transmission lines, or marine structures, uplift capacity governs the design. Analytical models and empirical rules typically are utilized to estimate uplift capacity. However, for stability and safety, the ultimate capacity is commonly verified by undertaking a pile load test program. The term “failure load” or “interpreted failure load” is then evaluated from the result of a load test. Over the years, numbers of interpretation criteria have been proposed [2-9] for interpreting the failure load. However, these methods are generally applied on compression load tests. Research on the evaluation of compression interpretation criteria has been conducted for driven piles [10-13] and drilled shafts [8, 9, 13, 14] while other researchers [15-17] studied uplift interpretation criteria for drilled shafts. Hussein and Sheahan [18] utilized compression interpretation criteria for driven pile uplift analysis. Recent studies present [19, 20] a number of uplift interpretation criteria for belled piers. However, most interpretation criteria are meant for compression load test data because there is a lack of universally accepted procedure for uplift static load test result assessment [18] . Therefore, an evaluation on the applicability of available interpretation criteria using uplift load test data is

* Corresponding author. E-mail address: yjc@cycu.edu.tw
Tel.: +886-3-2654227

indeed essential. Likewise, it is worth to evaluate various interpretation criteria utilizing a database of driven PC piles under uplift conditions to have a straightforward, clear, simple and direct criterion that can consistently be used on a larger range of uplift load tests. Moreover, capacity approximation from the interrelationships of the representative criteria will be derived for driven PC pile design.

Table 1 lists the representative interpretation methods for examination to evaluate their applicability on uplift interpreted capacity and their interrelationships as well. The L_1-L_2 method [8-9, 15] and Slope tangent method [21] which were developed for drilled shafts are adopted in this study to evaluate their suitability in driven piles. A wide range of data on axial uplift static load tests on driven piles for both drained and undrained loading conditions is utilized. The piles are round and square cross section which were installed using drop, air or steam, diesel, and hydraulic hammers. The installation methods were incorporated to examine the influence of hammer types. To derive recommendations helpful for geotechnical practice, results are statistically and graphically compared.

Table 1 Definition of representative uplift interpretation criteria for driven PC piles [12]

Method	Category	Definition of interpreted capacity, *Q*
Van der Veen (1953)	Mathematical model	Q_{VDV} is P_{ult} that gives a straight line when log (1-P/P_{ult}) is plotted versus total displacement.
Chin (1970)	Mathematical model	Q_{CHIN} is the inverse slope (1/m) of a line s/p = ms+c, where p = load and s = total displacement.
Fuller and Hoy (1970)	Settlement limit	$Q_{F\&H}$ is the minimum load that occurs at a rate of total displacement of 0.05 in. per ton (0.14 mm/kN).
DeBeer (1970)	Settlement limit	Q_{DB} is the load at the change in slope on a log-log load- displacement curve.
Davisson (1972)	Graphical construction	Q_{DAV} occurs at a displacement equal to the pile elastic compression line (PD/AE) offset by 0.15 in. (3.8 mm), where P = load, D = depth, A = area, E = Young's modulus.
Slope tangent (O'Rourke and Kulhawy 1985)	Graphical construction	Q_{ST} occurs at a displacement equal to the initial slope of the load-displacement curve offset by 0.15 in. (3.8 mm).
L_1 - L_2 (Hirany and Kulhawy, 1988, 1989, 2002)	Graphical construction	Q_{L1} and Q_{L2} correspond to elastic limit and failure threshold loads, respectively as shown in Fig. 1

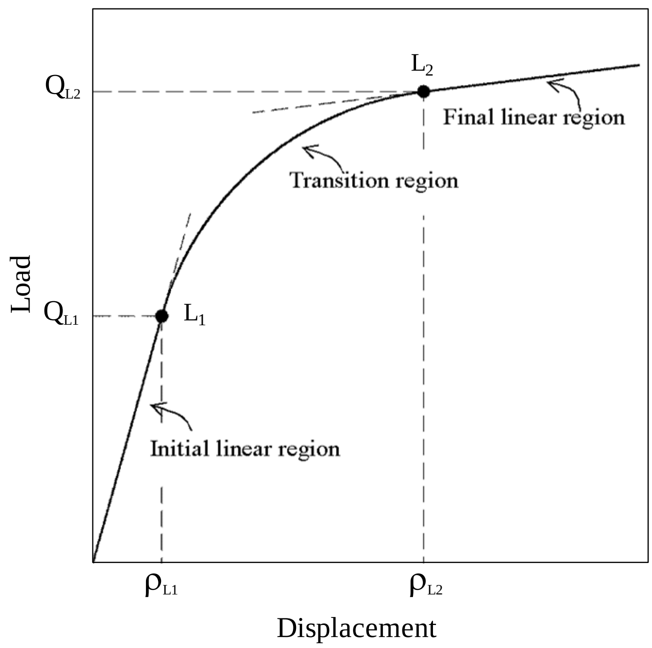

Fig. 1 Regions of load-displacement curve [12]

2. Load Test Database

This study compiled static uplift load test results on straight-sided driven PC piles that were obtained mainly from available test reports and geotechnical literature. The developed database contained 27 sites with 80 field uplift load tests covering a wide variety of pile shapes, soil profiles, and construction methods. The soil profile is grouped herein as "drained loading condition” and “undrained loading condition” which is based on the governing state of soil along the pile depth [12]. Using the round and square cross-sections as well as the drained and undrained loading, four groups were developed namely drained uplift round piles (DUR), drained uplift square piles (DUS), undrained uplift round piles (UUR), and undrained uplift square piles (UUS). The DUR has 7 sites with 27 tests, DUS has 10 sites with 31 tests, UUR has 3 sites with 11 tests and UUS has 7 sites with 11 tests. Further subdivision was made based on hammer types for cases with driving data. There are 7, 13, and 26 tests using drop, air/steam, and diesel hammers, respectively for drained loading and there are 2, 4, 4, and 5 tests using drop, air/steam, diesel, and hydraulic hammers, respectively for undrained loading. Tables 2-5 summarize the basic information, driving data, and interpreted capacities for the four groups while Table 6 lists the sources of data. The summary of pile geometry and capacity with their coefficients of variation (COV) is in Table 7. In this table, somewhat comparable foundation dimensions are observed for both drained and undrained tests but the range of geometry is relatively wide. In addition, the pile capacities of undrained load tests are smaller than the drained load tests. This may be due to the limited numbers of data for undrained loading for comparison.

3. Load Test Interpretation

Table 1 presents the seven interpretation criteria for evaluation which were chosen because they illustrate the lower, middle, and higher bounds criteria based on practice. These criteria interpret capacity Q from load-displacement curve of each pile. Marcos et.al [12] discussed the definitions of interpreted capacity of the selected criteria and the details of the development of these criteria are found elsewhere [2, 4-9, 15, 21].

Table 2 Basic information and interpreted results for drained uplift round section (DUR) test

Site & Pile no.	Test site/ Soil description	GWT[a] (m)	D_r[b] (%)	Pile depth/dia. (m)	Hammer type[c] /energy[g] (kN-m)	Final set[h] (bl/25mm)	Interpreted capacity, Q[j] (kN)							
							Q_{L1}	Q_{DB}	Q_{ST}	Q_{DAV}	Q_{L2}	$Q_{F\&H}$	Q_{VDV}	Q_{CHIN}
DUR1	Spain; fine silty sand	0	65	18.0/0.91	--[d]	--[d]	1235	1829	1620	900	2147	2500	2555	3239
DUR2-1	Miliao, Taiwan; silty sand	1.9	52	25.0/0.50	C / --[d]	2[e]	545	1400	1038	1180	1500	1700	1610	1927
DUR2-2			52	27.0/0.50	C / --[d]	2[e]	750	1389	1370	1463	1875	2050	1998	2486
DUR2-3			52	23.0/0.50	C / --[d]	2[e]	625	800	962	1035	1172	1380	1250	1491
DUR2-4			52	23.0/0.40	C / --[d]	2[e]	220	490	520	532	560	535	580	686
DUR2-5			53	12.0/0.50	C / --[d]	2[e]	450	800	868	750	1020	1020	1046	1220
DUR2-6			52	23.0/0.50	C / --[d]	2[e]	421	1000	1120	1135	1600	1526	1610	1812
DUR2-7			52	23.0/0.50	C / --[d]	2[e]	597	1000	1060	1060	1500	1500	1627	1852
DUR2-8			52	25.0/0.50	C / --[d]	2[e]	579	1490	1245	1510	1912	1888	1951	2144
DUR2-9			53	12.0/0.50	C / --[d]	2[e]	326	875	962	730	1123	1123	1161	1381
DUR2-10			53	11.0/0.50	C / --[d]	2[e]	800	1260	1240	1015	1842	1804	1843	2211
DUR3	Kaohsiung,Taiwan;clayey silty sand	--[d]	32	20.0/0.60	C / --[d]	2[e]	750	980	1220	1215	1563	1500	1591	1764
DUR4-1	Dramen, Norway; uniform loose normally consolidated sand	1.7	9	8.0/0.28	A / 7.5	2[e]	53	83	89	88	87	86	92	110
DUR4-2			8	16.0/0.28	A / 7.5	4[e]	129	205	238	232	272	238	277	299
DUR4-3			22	23.5/0.28	A / 7.5	8	100	200	229	213	294	264	329	381
DUR 5-1	Port of Santos, Brazil; clayey silty sand	0	39	41.0/0.90	B / --[d]	7	500	1300	1760	1905	2010	2035	2150	2900
DUR 5-2			39	41.0/0.90	B / --[d]	83	610	1200	1500	1600	2020	2035	2036	2758
DUR6-1	Vietnam; clayey sand	--[d]	45.2	20.4/0.60	C / --[d]	--[d]	1145	1150	2110[f]	2230[f]	2250[f]	2250[f]	2290	2320
DUR6-2	Vietnam; clayey sand		58.5	20.4/0.60	C / --[d]	--[d]	1035	1150	2350[f]	2475[f]	2500[f]	2506[f]	2541	2585
DUR6-3	Vietnam; silty clayey sand		41.7	20.4/0.60	C / --[d]	--[d]	720	1080	1290[f]	1300[f]	1310[f]	1290[f]	1310	1313
DUR7-1	Miliao, Taiwan; silty sand	1.9	52	23.0/0.50	C / 205.8	1	420	630	1122	1350	1403	>1521[i]	1590	1686
DUR7-2			52	9.0/0.50	C / 205.8	1	320	695	822	790	963	1080	1150	1208
DUR7-3			52	9.0/0.50	C / 205.8	1	305	740	880	840	1030	1080	1100	1252
DUR7-4			53	14.0/0.50	C / 205.8	1	318	900	1200	1275	1405	>1570[i]	1420	1756
DUR7-5			53	14.0/0.50	C / 205.8	1	421	930	1160	1175	1523	1717	1650	1899
DUR7-6			53	11.0/0.50	C / 205.8	1	320	1618	920	910	1618	1766	1755	2036
DUR7-7			52	23.0/0.50	C / 205.8	1	520	1200	1160	1270	1720	1864	1940	2055

[a] GWT = groundwater table; [b] Dr = relative density; if not reported, it is inferred from standard penetration test N value [3]; [c] A = drop hammer; B = air/steam hammer; C = diesel hammer; D = hydraulic hammer ; [d] -- not reported; [e] value is deduced based on available information; [f] interpreted capacity is deduced from hyperbolic method [22]; [g] hammer efficiency; [h] number of blows of pile hammer for final 25mm of driving; [i] load test was terminated before interpreted load; [j] Q_{DB} = DeBeer, Q_{ST} = slope tangent, Q_{DAV} = Davisson, $Q_{F\&H}$ = Fuller and Hoy, Q_{VDV} = Van der Veen, Q_{CHIN} = Chin

Table 3 Basic information and interpreted results for drained uplift square Section (DUS) tests

Site & Pile no.	Test site/Soil description	GWT[a] (m)	D_r[b] (%)	Pile depth/sec. (m)	Hammer type[c]/energy[g] (kN-m)	Final set[h] (bl/25mm)	Interpreted capacity, Q[j] (kN)							
							Q_{L1}	Q_{DB}	Q_{ST}	Q_{DAV}	Q_{L2}	$Q_{F\&H}$	Q_{VDV}	Q_{CHIN}
DUS1	Baghdad, Iraq; uniform sand with silt	5.7	43	11.0/0.285	C/33.6 e	4	195	255	395	405	425	450	560	561
DUS2	Canada; clayey silt & silty sand	9.8	41	14.7/0.305	C/62	6	127	138	193	183	283	262	338	351
DUS3	Bukit Timah, Singapore; residual soil	-- [d]	56	23.1/0.400	A/69	25	1138	1950	2000	2535	2560	2875	2850	3397
DUS4-1	Florida, USA; calcareous silty sand and sandy clay	0	41	19.4/0.762	B/122	13	2356	3000	4003	4003	>4003[i]	>4003[i]	5000	5872
DUS4-2			25	16.7/0.610	B/122	9	1779	2002	2200	2258	2650	2733	2872	2903
DUS4-3			44	20.1/0.762	B/122	9	2258	2669	3800	4003	>4003[i]	>4003[i]	4004	5454
DUS4-4			44	20.4/0.762	B/122	8	2272	2450	3890	3810	>4195[i]	>4195[i]	4400	5789
DUS4-5			22	15.8/0.610	B/122	2	1602	1710	2015	1960	2334	2308	2363	2484
DUS4-6			25	16.4/0.610	B/122	2	1661	2003	2250	2345	2522	2520	2534	2773
DUS4-7			28	17.7/0.762	B/122	2	1344	1650	1710	1500	2515	2455	2690	2821
DUS4-8			15	13.8/0.610	B/122	1	389	1000	890	830	1334	1261	1335	1429
DUS4-9			15	13.5/0.610	B/122	1	515	800	820	774	1112	1076	1112	1194
DUS4-10			25	14.1/0.762	B/122	1	445	1334	1000	980	1407	1398	1335	1491
DUS4-11			28	17.7/0.610	B/122	1	1500	2225	3610[f]	3875[f]	4400[f]	>2847[i]	6320	6591
DUS5-1	Sao Paulo, Brazil; sandy soil	-- [d]	22	12.0/0.170	-- [d]	-- [d]	10	17	18	16	20	>25[i]	22	26
DUS5-2			22	12.0/0.170	-- [d]	-- [d]	25	35	41	41	44	>50[i]	43	50
DUS5-3			22	12.0/0.170	-- [d]	-- [d]	40	50	59	58	60	>65[i]	62	66
DUS5-4			22	12.0/0.170	-- [d]	-- [d]	25	40	50	49	52	>54[i]	51	55
DUS6-1	Westminster, California; soft to dense, intermixed silty sands, silts and clay	3.1	56	15.2/0.356	-- [d]	-- [d]	279	440	600	720	930	965	980	1045
DUS6-2			56	15.1/0.356	-- [d]	-- [d]	249	445	590	690	899	968	995	1072
DUS6-3			56	17.7/0.356	-- [d]	-- [d]	209	334	540	624	943	943	1015	1147
DUS6-4			56	17.4/0.356	-- [d]	-- [d]	222	310	540	615	780	>885[i]	885	1002
DUS7-1	Palo-Verde California; soft to dense sands, silts and clay	4.6	54	11.6/0.356	-- [d]	-- [d]	234	356	441	433	507	500	520	575
DUS7-2			54	12.2/0.356	-- [d]	-- [d]	356	510	810[f]	862[f]	865[f]	993[f]	1060	1155
DUS7-3			54	12.2/0.356	-- [d]	-- [d]	295	310	600[f]	568[f]	700[f]	735[f]	802	915
DUS8-1	India; sandy silt	below tip	15	3.0/0.200	A/2.5	8	10	23	24	20	32	>35[i]	35	39
DUS8-2			15	3.0/0.200	A/2.5	14	9	20	24	21	32	>35[i]	35	39
DUS8-3			15	3.0/0.200	A/2.5	14	12	18	28	26	39	>44[i]	44	45
DUS9-1	Florida, USA; clayey sand	-- [d]	-- [d]	23.5/0.356	C/54.2	2	200	250	600[f]	650[f]	702[f]	722[f]	778	851
DUS9-2			-- [d]	16.2/0.457	C/54.2	7	215	278	381	347	393	>400[i]	421	616
DUS10	South Carolina, USA; fine silty sand	1.1	39	17.0/0.305	C/35.7	8	288	890	1281	1168	1735	1246	1743	1780

[a] GWT = groundwater table; [b] Dr = relative density; if not reported, it is inferred from standard penetration test N value [3]; [c] A = drop hammer; B = air/steam hammer; C = diesel hammer; D = hydraulic hammer ; [d] -- not reported; [e] value is deduced based on available information; [f] interpreted capacity is deduced from hyperbolic method [22]; [g] hammer efficiency; [h] number of blows of pile hammer for final 25mm of driving; [i] load test was terminated before interpreted load; [j] Q_{DB} = DeBeer, Q_{ST} = slope tangent, Q_{DAV} = Davisson, $Q_{F\&H}$ = Fuller and Hoy, Q_{VDV} = Van der Veen, Q_{CHIN} = Chin

Table 4 Basic information and interpreted results for undrained uplift round section (UUR) tests

Site & Pile no.	Test site/Soil description	GWT[a] (m)	s_u[b] (kN/m^2)	Pile depth/dia. (m)	Hammer type[c]/energy[g] (kN-m)	Final set[h] (bl/25mm)	Interpreted capacity, Q[i] (kN)							
							Q_{L1}	Q_{DB}	Q_{ST}	Q_{DAV}	Q_{L2}	$Q_{F\&H}$	Q_{VDV}	Q_{CHIN}
UUR1-1	Negeri Sembilan, Malaysia; clay	-- [d]	15.8	17.5/0.50	D/88 [e]	-- [d]	203	585	497	415	651	686	745	868
UUR1-2			15.8	17.5/0.50	D/88 [e]	-- [d]	470	545	962	1010	1106	>1241[f]	1350	1504
UUR1-3			15.8	7.5/0.50	D/88 [e]	-- [d]	87	200	274	210	355	333	370	413
UUR2-1	Bangkok, Thailand; soft clay	1.75	25.6	20.0/0.40	A/59 [e]	-- [d]	225	275	305	324	424	399	402	451
UUR2-2			25.6	20.0/0.40	A/59 [e]	-- [d]	71	107	148	155	204	172	210	232
UUR3-1	China; silty clay	-- [d]	-- [d]	43.0/0.50	C/-- [d]	-- [d]	355	520	735	768	760	>820[f]	900	1543
UUR3-2			-- [d]	43.0/0.50	C/-- [d]	-- [d]	355	410	680	757	760	>820[f]	910	1072
UUR3-3			-- [d]	43.0/0.60	C/-- [d]	-- [d]	310	385	642	757	745	>820[f]	950	1017
UUR3-4			-- [d]	43.0/0.60	C/-- [d]	-- [d]	529	700	842	810	1133	>1200[f]	1310	1588
UUR3-5			-- [d]	43.0/0.60	C/-- [d]	-- [d]	405	590	960	1078	1163	1240	1275	1531
UUR3-6			-- [d]	43.0/0.60	C/-- [d]	-- [d]	395	800	978	1100	1169	1240	1260	1539

[a] GWT = groundwater table; [b] s_u = undrained shear strength; if not reported, it is inferred from standard penetration test N value [3]; [c] A = drop hammer; B = air/steam hammer; C = diesel hammer; D = hydraulic hammer; [d] not reported; [e] value is deduced based on available information; [f] load test was terminated before interpreted load; [g] hammer efficiency; [h] number of blows of pile hammer for final 25mm of driving; [i] Q_{DB} = DeBeer, Q_{ST} = slope tangent, Q_{DAV} = Davisson, $Q_{F\&H}$ = Fuller and Hoy, Q_{VDV} = Van der Veen, Q_{CHIN} = Chin

Table 5 Basic information and interpreted results for undrained uplift square section (UUS) tests

Site & Pile no.	Test site/Soil description	GWT[a] (m)	s_u[b] (kN/m^2)	Pile depth/ sec. (m)	Hammer type[c]/energy[g] (kN-m)	Final set[h] (bl/25mm)	Interpreted capacity, Q[i] (kN)							
							Q_{L1}	Q_{DB}	Q_{ST}	Q_{DAV}	Q_{L2}	$Q_{F\&H}$	Q_{VDV}	Q_{CHIN}
UUS1	Mexico; clayey soil	2	34	15.0/0.300	-- [d]	-- [d]	107	300	252	165	395	376	500	615
UUS2-1	Canada-Site A; firm to stiff glacial clay	-- [d]	-- [d]	25.0/0.380	C/69	15	200	410	680	655	700	710	720	768
UUS2-2			-- [d]	23.8/0.380	C/69	15	330	510	710	710	710	710	770	844
UUS3	Canada-Site B; soft to firm marine silt	-- [d]	-- [d]	47.2/0.380	C/69	15	296	410	710	>710 [e]	>710 [e]	>710 [e]	910	1454
UUS4	Louisiana; deltaic clays and silt	-- [d]	154	25.0/0.356	B/-- [d]	-- [d]	360	510	560	596	552	623	624	630
UUS5-1	Illinois, Carbondale; silty clay	1.52	73.4	6.4/0.305	B/-- [d]	-- [d]	125	320	330	323	395	391	397	418
UUS5-2			73.4	6.4/0.305	B/-- [d]	-- [d]	145	311	316	210	317	313	353	424
UUS5-3			73.4	6.4/0.305	B/-- [d]	-- [d]	110	175	208	193	205	205	250	297
UUS6-1	Kinnegar N. Ireland; clayey silt	-- [d]	24.2	6.0/0.250	D/22	-- [d]	24	51	63	60	64	53	66	74
UUS6-2			24.2	6.0/0.250	D/22	-- [d]	23	56	60	57	61	54	62	66
UUS7	Egypt; sandy clay	-- [d]	NR	11.6/0.320	C/74	3	193	240	461[f]	400	525[f]	>400 [e]	627	757

a GWT = groundwater table; b su = undrained shear strength; if not reported, it is inferred from standard penetration test N value [3]; c A = drop hammer; B = air/steam hammer; C = diesel hammer; D = hydraulic hammer; d -- not reported; e load test was terminated before interpreted load; f interpreted capacity is deduced from hyperbolic method [22]; g hammer efficiency; h final set = number of blows of pile hammer for final 25mm of driving; i QDB = DeBeer, QST = slope tangent, QDAV = Davisson, QF&H = Fuller and Hoy, QVDV = Van der Veen, QCHIN = Chin

Tables 2-5 present interpretation results for the DUR, DUS, UUR, and UUS tests, respectively. A number of tests were stopped prior to attaining the interpreted capacities. Based on the observation of all the load test results, some tests reached failure at displacements of less than 5 mm. In addition, many of these tests yielded maximum displacements of less than 20 mm. Therefore, for cases with maximum displacements of < 5 mm, the hyperbolic method [22] was used to infer the interpreted load. However, for a more reasonable extrapolation of uplift capacity, the interpreted displacement was limited to 15 mm. Beyond this displacement, the capacity was not extrapolated but instead denoted as greater than (>) the maximum applied load. Further, by definition, the capacity by Van der Veen and Chin methods can be larger than the maximum applied load. The values with > signs were disregarded in the statistical analysis to avoid prejudice.

4. Drained Load Test Evaluation Results

The drained uplift test summary showing the statistics of interpreted capacities and displacements of the DUR, DUS, and all drained data combined are given in Tables 8 and 9, respectively. To evaluate the interrelationship, characteristics, and applicability of the methods, results are compared from the statistical data presented. For a number of cases, Q_{VDV} are above the maximum applied load and so for these cases, the displacement were not extrapolated which resulted to fewer "n" values for Q_{VDV} as presented in Tables 9 and 11. Note that Q_{L1} is not an interpreted failure load or capacity but an elastic limit, and is included herein as reference only.

Table 8 shows the results of mean load ratios with Q_{CHIN} as the reference. For round piles, mean load ratios range from 0.59 to 0.87 and 0.52 to 0.90 for square piles. The COV values are 8 to 24% for round and 6 to 32% for square. In general, the mean load ratios of square piles are slightly larger than for round piles. From these results, Q_{DB} shows the smallest mean value and Q_{VDV} has the largest value. Q_{CHIN} is always beyond and above the actual field measurement. The Fuller and Hoy method interpreted relatively few load test cases for square piles and this can be attributed to its definition. Table 9 shows that Q_{L1} exhibited the lowest mean ratio and displacement. This means that the initial linear region develops at very small displacement. The mean ratio statistics present that lower value of displacements give higher coefficient of variation (COV). This may be caused by fluctuation during the initial loading. Other reason may be the possible sensitivity in measurement. Table 9 shows the mean uplift displacements for round and square piles and it follows the same order as the capacities. The range of displacement at the interpreted capacity for round piles range from 5.5 mm or 1.1%B at Q_{DB} to 18.1 mm or 3.7%B at Q_{L2} to >33.2 mm or >7%B for Q_{CHIN} and the square section piles range from 3.6 mm or 0.92%B at Q_{DB} to 17.9 mm or 4.8%B at Q_{L2} to >26.8 mm or 8.5%B for Q_{CHIN}. A high COV values for the mean displacement data is noted which range from 24 to 64% (round) and 24 to 67% (square).

Table 6 Reference sources of pile load tests in Tables 2-5

Pile no.	Reference source
DUR1	M. R. Oteo, C. S. Sanches, J. R. Del, and A. Soriano, "Field testing on large driven piles," Proc. 11th International Conference on Soil Mechanics and Foundation Engineering, San Francisco, vol. 3, pp. 1559-1564, 1985.
DUR2, DUR3	C. H. Chen, T. D. Perng, J. H. Hwang, and L. T. Chang, "Analyses for load test data of PC piles on West-Coast reclaimed areas of Taiwan," Journal of the Chinese Institute of Civil and Hydraulic Engineering, vol. 12, no. 1, pp. 51-62, 2000.
DUR4	O. S. Gregersen,, G. Aas,, and E. D. Biagio, "Load tests on friction piles in loose sand," Proc. 8th International Conference on Soil Mechanics and Foundation Engineering, vol. 2, pp. 109-117, 1973.
DUR5	S. Niyama, Jr. Azevedo, N. C. M. Polla, L. F. A. Souza, and M. A. Dechichi, "Drivability and performance assessment of driven piles subjected to negative skin friction," International Symposium on Pile Driving, 2011.
DUR6	Sinotech Engineering Consultants, Limited, "Load test report of utility plant," Vietnam, 2011.
DUR 7	Diagnostic Engineering Consultants, Ltd. "Report on driven pile load tests for petroleum factory project," Taiwan, 1997.
DUS1	A. Altaee, B. H. Fellenius, and E. Evgin, "Axial load transfer for piles in sand: I. Tests on an instrumented precast pile," Canadian Geotechnical Journal, vol. 29, no. 1, pp. 11-20,1992.
DUS2	C. D. Thompson,, and M. Devata, "Evaluation of ultimate bearing capacity of different piles by wave equation analysis." Proc. International Seminar on the Application of Stress-Wave Theory on Piles, pp. 163-195, 1980.
DUS3	C. E. Ho, "Evaluation of the ultimate uplift capacity of piles," Proc. 30th Year Anniversary Symposium of the Southeast Asian Geotechnical Society, Bangkok Thailand, 1997.
DUS4	M. H. Hussein, J. M. Sheahan. "Uplift capacity of driven piles from static loading tests," Proc. 3rd International Conference on Case Histories in Geotechnical Engineering, St. Louis, Missouri, June 1993.
DUS5	S. M. Menezes, D. de Carvalho, and da Rocha de P. J. Albuquerque, "Analysis of uplift loads of precast-concrete piles in porous soils," Exacta, vol. 4, no. 1, pp. 191-200, 2006.
DUS6-DUS7	K. D. Tucker, "Uplift capacity of pile foundations using CPT data," Proc. In-situ '86, Geotechnical Special Publications, no. 6, 1986, pp. 1077-1093.
DUS8	B. G. Rao, M. P. Jain, and G. Ranjan, "Behaviour of spliced piles- A field study," Proc. Symposium on Prediction versus Performance in Geotechnical Engineering, 1992, pp. 27-44.
DUS9,UUS7	J. R. Davie, L. W. Young, and M. R. Lewis, "Uplift load tests on driven piles." Proc. 3rd International Conference on Case Histories in Geotechnical Engineering, 1993.
DUS10	C. L. Crowther, "Load testing of deep foundations-the planning, design, and conduct of pile load tests," A Wiley-Interscience Publication, pp. 120-134, 1988.
UUR1	S. Krishnan and L. S. Kai, "A novel approach to the performance evaluation of driven prestressed concrete piles and bored cast-in-place piles," Proc. 10th International Conference on Piling and Deep Foundations, pp. 1-9, 2006.
UUR2	B. Indraratna, A. S. Balasubramaniam, P. Phamvan, and Y. K. Wong, "Development of negative skin friction on driven piles in soft Bangkok clay." Canadian Geotechnical Journal, vol. 29, no. 3, pp. 393-404, 1992.
UUR3	L. Ying, and G. F. Jin, "Uplift behavior and load transfer mechanism of prestressed high-strength concrete piles." Journal of Central South University of Technology, vol. 17, no.1, pp. 136-141, 2010.
UUS1	A. P. Jaime, M. P. Romo, J. A. Ponce, and A. M. Mitre, "Static tests on friction piles in Mexico clay." Proc. 12th International Conference on Soil Mechanics and Foundation Engineering, vol. 2, pp. 1141-1146, 1989.
UUS2-UUS3	A. Sy, D. Siu, and B. F. Fellenius, "A case history of prestressed concrete pile splices problems." Proc. 4th International Conference on the Application of Stress-Wave Theory to Piles, 1992, pp. 479-486.
UUS4	Y. A. Hegazy, A. G. Cushing, and, C. J. Lewis, "Driven pile capacity in clay and drilled shaft capacity in rock from field load tests." Proc. 5th International Conference on Case Histories in Geotechnical Engineering, 2004 , pp. 1-8.
UUS5	S. Kumar, C. Alarcon, B. R. Schmitt, and D. Kort, "Construction and full-scale testing of precast concrete piles made with coal combustion products," Electronic Journal of Geotechnical Engineering, Vol. 10, No. A1, January, 2005.
UUS6	B. M. Lehane, R. J. Jardine, and B. A. McCabe, "Pile group tension cyclic loading: Field test programme at Kinnegar N. Ireland," Health and Safety Executive Research Report RR101, 2003.

Table 7 Range of geometry of driven piles for analysis

Data	Number of tests	Statistics	Pile geometry (m)		D/B	Interpreted capacity, Q_{L2}, (kN)
			Depth, D	Diameter[a], B		
DUR	27	Range	8.0-41.0	0.28-0.91	18.0-83.9	87-2500
		Mean	19.8	0.53	38.6	1416
		COV	0.42	0.30	0.40	0.43
DUS	31	Range	3.0-23.5	0.17-0.76	15.0-70.6	20-4400
		Mean	14.5	0.43	38.3	1048
		COV	0.35	0.48	0.47	1.03
UUR	11	Range	7.5-43.0	0.40-0.60	15.0-86.0	204-1169
		Mean	31.0	0.51	59.8	770
		COV	0.46	0.14	0.41	0.45
UUS	11	Range	6.0-47.2	0.25-0.38	21-124.2	61-710
		Mean	16.3	0.32	47.3	392
		COV	0.80	0.15	0.68	0.60

[a] or width of square section

Table 8 Summary of interpreted capacities for drained uplift tests

Pile section	Data	Interpreted Q/Q_{CHIN}							
		Q_{L1}	Q_{DB}	Q_{ST}	Q_{DAV}	Q_{L2}	$Q_{F\&H}$	Q_{VDV}	Q_{CHIN}
Round (DUR)	n[a]	27	27	27	27	27	25	27	27
	Mean	0.31	0.59	0.66	0.67	0.82	0.84	0.87	1.00
	SD	0.10	0.11	0.13	0.16	0.08	0.08	0.07	-
	COV	0.33	0.19	0.20	0.24	0.09	0.09	0.08	-
Square (DUS)	n[a]	31	31	31	31	28	18	31	31
	Mean	0.36	0.52	0.67	0.68	0.84	0.87	0.90	1.00
	SD	0.13	0.17	0.10	0.11	0.08	0.05	0.07	-
	COV	0.36	0.32	0.16	0.16	0.10	0.06	0.08	-
All Data	n[a]	58	58	58	58	55	43	58	58
	Mean	0.34	0.55	0.67	0.67	0.83	0.85	0.89	1.00
	SD	0.12	0.15	0.12	0.13	0.08	0.07	0.07	-
	COV	0.36	0.27	0.17	0.20	0.10	0.08	0.08	-

[a] not including interpreted results with “>” symbo

Table 9 Summary of Interpreted Displacements for Drained Uplift Tests

Pile section	Data	Displacement at Interpreted Criteria (mm)							
		δ_{L1}	δ_{DB}	δ_{ST}	δ_{DAV}	δ_{L2}	$\delta_{F\&H}$	δ_{VDV}	δ_{CHIN}
Round (DUR)	n[a]	27	27	27	27	27	25	20 [b]	27
	Mean	1.7	5.5	7.1	7.7	18.1	21.5	30.5	>33.2
	SD	1.1	3.5	1.7	2.1	8.7	11.5	13.5	14.9
	COV	0.63	0.64	0.24	0.27	0.48	0.54	0.44	0.45
	δ/B (%)	0.34	1.1	1.4	1.5	3.7	4.1	6.4	>7.0
Square (DUS)	n[a]	31	31	31	31	28	18	16 [b]	31
	Mean	1.7	3.6	6.4	6.8	17.9	21.3	25.0	>26.8
	SD	1.1	2.4	1.5	3.0	10.6	9.9	12.2	12.9
	COV	0.65	0.67	0.24	0.44	0.60	0.47	0.49	0.48
	δ/B (%)	0.41	0.92	1.8	1.8	4.8	4.6	7.9	>8.5
All Data	n[a]	58	58	58	58	55	43	36 [b]	58
	Mean	1.7	4.4	6.7	7.2	18.0	21.4	28.1	>29.8
	SD	1.1	3.1	1.6	2.6	9.6	10.7	13.1	14.1
	COV	0.63	0.69	0.24	0.36	0.54	0.50	0.47	0.48
	δ/B (%)	0.38	1.0	1.6	1.7	4.2	4.3	7.1	>7.8

[a] not including interpreted results with “>” symbol
[b] “n” values for $\delta_{VDV} < Q_{VDV}$

The normalized load-displacement curves are shown in Fig 2. to better compare the criteria. The figure includes both round and square piles to assess the shape effects. The plot shows the relationship of mean ratio of each criterion to Q_{CHIN} and the mean displacement (δ) and displacement/diameter (δ/B) in Figs. 2(a) and 2(b), respectively. Comparison of the normalized curves in Fig. 2(a) demonstrates somewhat stiffer response for square piles while Fig. 2(b) for the normalized displacement indicates good agreement between round and square piles. The slightly stiffer behavior of square piles in Fig. 2(a) might result from the somewhat better frictional resistance of square pile edges against uplift loads. Other reason may be the differences in database. However, the difference is significantly small. For both pile sections, the criteria found within the L_1 to L_2 transition are DeBeer, slope tangent, and Davisson, while Fuller and Hoy and Van der Veen are beyond the failure threshold.

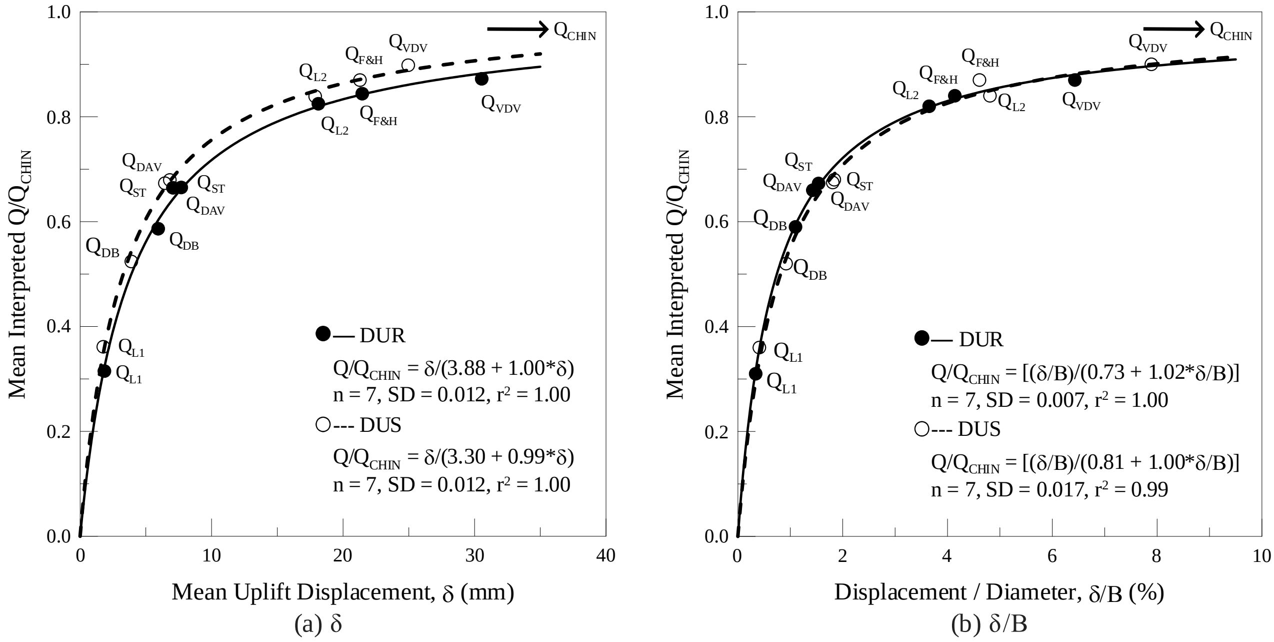

Fig. 2 Mean load-displacement comparison for drained uplift loading using

Points L_1 and L_2 cover the significant portions of the curve which can be a good reference for the criteria. These points can provide approximations of capacity because they illustrate the typical order relationships among the criteria [12]. To exhibit this relationships, round and square drained data are combined (Table 8) because their difference is small as discussed above. The drained loading capacity using L_1 are: Q_{DB} = 1.6 Q_{L1}, Q_{ST} = 2.0 Q_{L1}, Q_{DAV} = 2.0 Q_{L1}, Q_{L2} = 2.4 Q_{L1}, Q_{FH} = 2.5 Q_{L1}, Q_{VDV} = 2.6 Q_{L1}, Q_{CHIN} = 2.9 Q_{L1}. The drained loading capacity using L_2 are: Q_{DB} = 0.66 Q_{L2}, Q_{ST} = 0.81 Q_{L2}, Q_{DAV} = 0.76 Q_{L2}, Q_{FH} = 1.02 Q_{L2}, Q_{VDV} = 1.07 Q_{L2}, Q_{CHIN} = 1.20 Q_{L2}. These proportions can be adopted when needed, such as when load test data are limited or when the tests are stopped at an early stage.

5. Undrained Load Tests Evaluation Results

Following the same approach as in drained load tests, the undrained uplift test summary showing the statistics of interpreted capacities and displacements of the UUR, UUS, and all drained data combined are given in Tables 10 and 11, respectively.

Table 10 Summary of interpreted capacities for undrained uplift tests

Pile section	Data	Interpreted Q/Q_{CHIN}							
		Q_{L1}	Q_{DB}	Q_{ST}	Q_{DAV}	Q_{L2}	$Q_{F\&H}$	Q_{VDV}	Q_{CHIN}
Round (UUR)	n[a]	11	11	11	11	11	6	11	11
	Mean	0.30	0.46	0.61	0.63	0.76	0.81	0.84	1.00
	SD	0.08	0.11	0.06	0.11	0.12	0.05	0.09	-
	COV	0.26	0.23	0.10	0.17	0.15	0.06	0.11	-
Square (UUS)	n[a]	11	11	11	10	10	9	11	11
	Mean	0.32	0.61	0.74	0.70	0.81	0.81	0.87	1.00
	SD	0.11	0.19	0.17	0.21	0.11	0.13	0.10	-
	COV	0.33	0.31	0.23	0.30	0.14	0.16	0.11	-
All Data	n[a]	22	22	22	21	21	15	22	22
	Mean	0.31	0.53	0.67	0.66	0.78	0.81	0.86	1.00
	SD	0.09	0.17	0.14	0.17	0.11	0.10	0.10	-
	COV	0.30	0.32	0.21	0.25	0.15	0.12	0.11	-

[a] not including interpreted results with “>” symbol

Table 10 shows the results of mean load ratios with Q_{CHIN} as the reference. For round piles, mean load ratios range from 0.46 to 0.84 and 0.61 to 0.87 for square piles. The COV values are 6 to 23% for round and 11 to 31% for square. As with drained loading, the same trend is observed from the methods which are relatively wide. Similarly, the Fuller and Hoy method interpreted few load test cases and the mean load ratios of square piles are generally larger than those for round piles.

Table 11 Summary of interpreted displacements for undrained uplift tests

Pile section	Data	Displacement at Interpreted Criteria (mm)							
		δ_{L1}	δ_{DB}	δ_{ST}	δ_{DAV}	δ_{L2}	$\delta_{F\&H}$	δ_{VDV}	δ_{CHIN}
Round (UUR)	n[a]	11	11	11	11	11	6	5[b]	11
	Mean	1.7	3.6	6.9	8.0	14.0	15.1	22.4	>21.2
	SD	0.8	1.8	1.6	2.6	4.2	5.4	5.1	6.7
	COV	0.49	0.50	0.24	0.32	0.30	0.36	0.23	0.32
	δ/B (%)	0.55	1.1	2.2	2.5	4.3	4.4	6.7	>6.4
Square (UUS)	n[a]	11	11	11	10	10	9	7[b]	11
	Mean	1.2	3.6	6.4	5.7	10.9	9.9	20.1	>22.8
	SD	0.68	2.2	1.8	1.9	6.6	6.2	6.7	13.0
	COV	0.55	0.60	0.29	0.33	0.61	0.62	0.33	0.57
	δ/B (%)	0.39	1.2	2.0	1.8	3.6	3.1	6.7	>7.5
All Data	n[a]	22	22	22	21	21	15	12[b]	22
	Mean	1.5	3.6	6.7	6.9	12.5	12.0	21.1	>22.0
	SD	0.77	1.9	1.7	2.5	5.6	6.2	6.0	10.1
	COV	0.53	0.54	0.26	0.36	0.44	0.52	0.28	0.46
	δ/B (%)	0.47	1.1	2.1	2.2	3.9	3.6	6.7	>6.9

[a] not including interpreted results with ">" symbol, [b] "n" values for $\delta_{VDV} < Q_{VDV}$

From these results, Q_{DB} shows the smallest mean value and Q_{VDV} has the largest value. Q_{CHIN} is always beyond and above the actual field measurement. Table 11 shows that Q_{L1} exhibited the lowest mean ratio and displacement. As in drained loading, the mean ratio statistics present that lower value of displacements gives higher coefficient of variation (COV) which implies that during the initial loading, greater variations in the behavior of load-displacement can be expected. Table 11 shows the mean uplift displacements for round and square piles and it follows similar pattern as the capacities. For round piles, the displacements at the interpreted capacity range from 3.6 mm or 1.1%B at Q_{DB} to 14.0 mm or 4.3%B at Q_{L2} to >21.2 mm or >6.4%B for Q_{CHIN}. For square piles, the displacements range from 3.6 mm or 1.2%B at Q_{DB} to 10.9 mm or 3.6%B at Q_{L2} to >22.8 mm or 7.5%B for Q_{CHIN}. The COV values for the mean displacement data range from 23 to 50% (round) and 29 to 60% (square).

The normalized load-displacement curves for round and square piles are shown in Figs. 3(a) and 3(b) using the mean displacement (δ) and displacement/diameter (δ/B), respectively. Both figures demonstrate that for round piles more ductile behavior is observed which may be due to several reasons. One possible reason is the relatively larger diameter of undrained-round piles in the database resulting to larger mean displacement to mobilize the capacity. Another reason could be the greater disturbance of the soil surrounding square piles during pile driving where the effect of pore water pressure is significant. Other reasons including pile set-up and database differences are possible. As in drained loading, the general trends of the interpretation criteria from the curves are similar. For both pile sections, the criteria found within the L_1 to L_2 transition are DeBeer, slope tangent, and Davisson, while Fuller and Hoy and Van der Veen are beyond the failure threshold.

The results of the adaptive Monte Carlo simulation are obtained by Kaymaz [17] by using the COMREL software. It is noted that the values of the reliability index are very close to each other for all methods under consideration. The AKA2PC method is much more accurate, where the coefficient Q^2 is closed to 1.This coefficient shows the goodness of kriging approximation with the technique of pilot points. Furthermore, Fig. 3 shows the accuracy of the approximation of the AKA2PC method, where the best approximation of the limit state function is performed by the AKA2PC with 12 additional pilot points and 05 confirmation simulation.

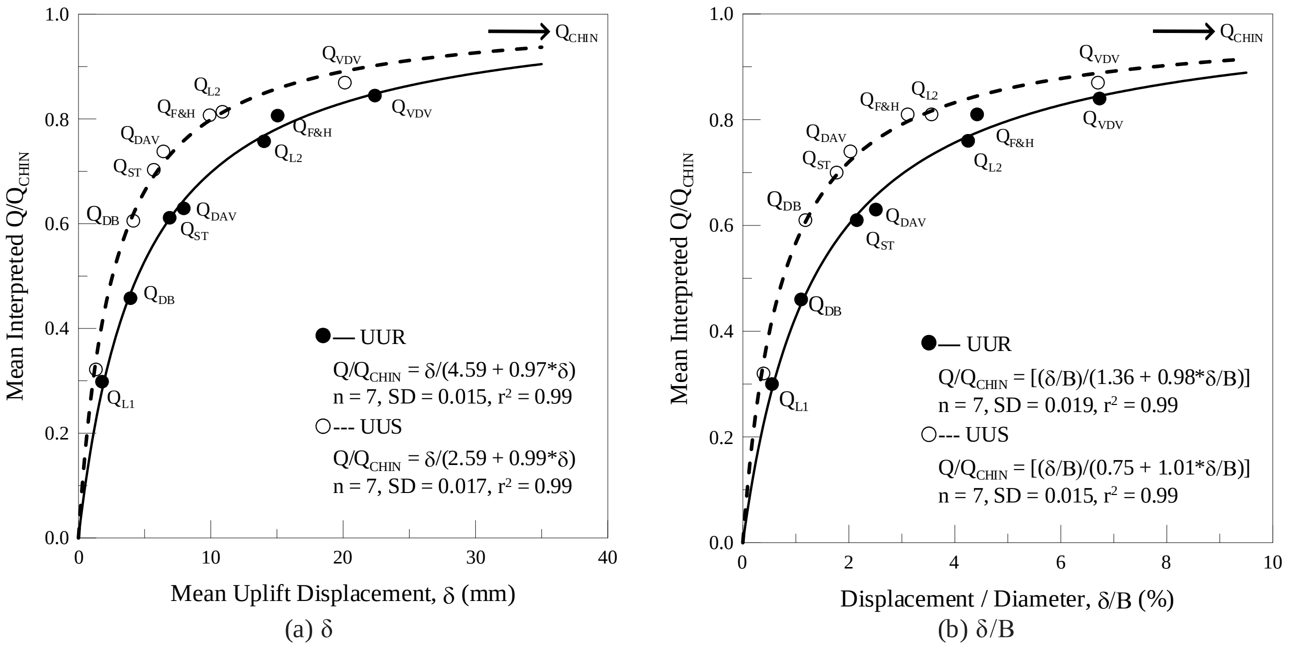

Fig. 3 Mean load-displacement comparison for undrained uplift loading using

Table 10 indicated the round and square undrained data. The undrained round piles capacity using L_1 are: Q_{DB} = 1.5 Q_{L1}, Q_{ST} = 2.0 Q_{L1}, Q_{DAV} = 2.1 Q_{L1}, Q_{L2} = 2.5 Q_{L1}, Q_{FH} = 2.7 Q_{L1}, Q_{VDV} = 2.8 Q_{L1}, Q_{CHIN} = 3.3 Q_{L1}. The undrained round piles capacity using L_2 are: Q_{DB} = 0.61 Q_{L2}, Q_{ST} = 0.80 Q_{L2}, Q_{DAV} = 0.83 Q_{L2}, Q_{FH} = 1.10 Q_{L2}, Q_{VDV} = 1.10 Q_{L2}, Q_{CHIN} = 1.32 Q_{L2}.

The undrained square piles capacity using L_1 are: Q_{DB} = 1.9 Q_{L1}, Q_{ST} = 2.3 Q_{L1}, Q_{DAV} = 2.2 Q_{L1}, Q_{L2} = 2.5 Q_{L1}, Q_{FH} = 2.5 Q_{L1}, Q_{VDV} = 2.7 Q_{L1}, Q_{CHIN} = 3.1 Q_{L1}. The undrained square piles capacity using L_2 are: Q_{DB} = 0.75 Q_{L2}, Q_{ST} = 0.91 Q_{L2}, Q_{DAV} = 0.86 Q_{L2}, Q_{FH} = 1.00 Q_{L2}, Q_{VDV} = 1.10 Q_{L2}, Q_{CHIN} = 1.23 Q_{L2}.

For convenience, the combined round and square undrained data using L_1 gives: Q_{DB} = 1.7 Q_{L1}, Q_{ST} = 2.2 Q_{L1}, Q_{DAV} = 2.1 Q_{L1}, Q_{L2} = 2.5 Q_{L1}, Q_{FH} = 2.6 Q_{L1}, Q_{VDV} = 2.8 Q_{L1}, Q_{CHIN} = 3.2 Q_{L1}. Using L_2, the capacity can be approximated for undrained loading as: Q_{DB} = 0.68 Q_{L2}, Q_{ST} = 0.86 Q_{L2}, Q_{DAV} = 0.85 Q_{L2}, Q_{FH} = 1.04 Q_{L2}, Q_{VDV} = 1.10 Q_{L2}, Q_{CHIN} = 1.28 Q_{L2}.

6. Drained and Undrained Load Tests Comparison

Drained and undrained load tests are compared and presented in Tables 8 to 11 and Fig. 4. From these illustrations, higher variability can be expected from undrained tests as evident in the generally larger standard deviation and coefficient of variation values in undrained tests. This may be due to the effect of pore water pressure in undrained soils during pile driving. In addition, drained loading capacity ratios are higher than undrained loading, but with small difference only. Further, drained tests displacements are somewhat higher, especially for larger values. Overall, for both drained and undrained loading, same general behavior is exhibited by the interpreted results of all criteria. With this, lower bound is represented by DeBeer method and is found within the nonlinear L_1 to L_2 transition, while upper bound is represented by Chin and is always above all measured results. Davisson and slope tangent are likewise located in the L_1 to L_2 region. Moreover, Van der Veen and Fuller and Hoy lies above or near L_2. The smallest COV's are given by L_2, Fuller and Hoy, and Van der Veen. On average, Q_{L1} = 0.33 Q_{CHIN} and Q_{L2} = 0.81 Q_{CHIN}.

The Chin method's displacements at interpreted capacity are >30 mm or >7.8%B (drained) and >25 mm or >6.9%B (undrained). The L_2, Fuller and Hoy, and Van der Veen methods' "failure" displacements are 18 to 30 mm or 4.2 to 7.2%B (drained) and 13 to 25 mm or 3.9 to 6.7%B (undrained), while the DeBeer, slope tangent, and Davisson methods have even lower "failure" displacements ranging from 5 to < 10 mm or 1 to 2%B. At L_1, the interpreted displacement is < 2 mm or <0.5%B.

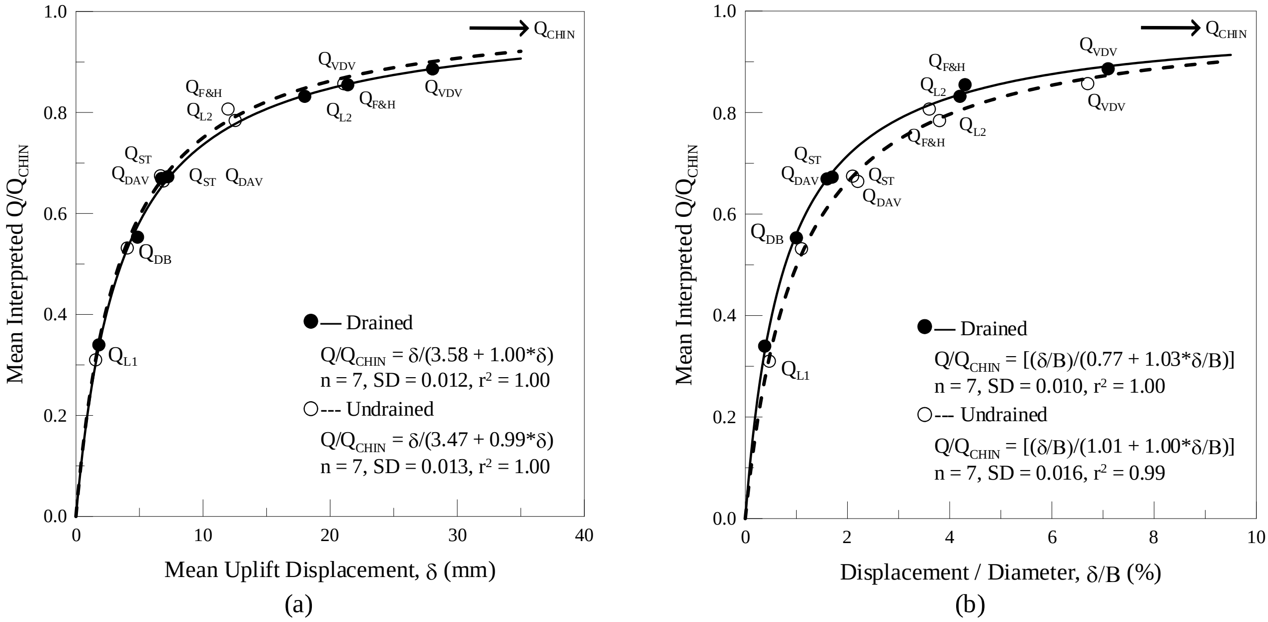

Fig. 4 Mean load-displacement comparison for drained and undrained uplift loading using (a) δ and (b) δ/B

7. Effects of Installation Methods on Driven Pile Performance

One important factor affecting the performance of driven piles is the method of installation. Drop, air/steam, diesel, and hydraulic hammers were used in the pile installation. Table 2-5 likewise show the subdivision of drained and undrained database by hammer type. This was done to assess the influence of hammer on the behavior of load-displacement.

7.2. Effects of hammer type driving on pile capacity

To analyze pile capacity during construction, the driving resistance which is expressed by blow count is used. The driving resistance is a function of hammer rated energy which is related to capacity. To explore this aspect, the database containing complete driving records were evaluated. However, because undrained load test cases have limited data, only drained tests were considered. Table 12 presents the ranges of hammer records. From the available air/steam hammer records, the rated energy is the same for the piles causing the non-existence of COV. For comparison, Engineering News (EN) formula was used for capacity prediction. The EN formula [23] was derived from work-energy theory and is given as:

$$Q_{EN} = W_r h/(s+C) \tag{1}$$

in which Q_{EN} = capacity of pile, W_r = ram weight, h = ram drop height, s = pile penetration/hammer blow, and C = constant. For single and double-acting hammers, the term Wr*h can be replaced by $E*E_H$, in which E = hammer efficiency and E_H = hammer rated energy.

To have a simple comparison, Q_{L2} is adopted. Table 13 and Fig. 6 show the comparison of predicted capacity (Q_{EN}) and measured capacity (Q_{L2}). The mean capacity ratios 1.5, 3.2, and 5.4 for drop, air/steam, and diesel hammers, respectively indicating an overestimation of the driving formula. The scatter in Fig. 6 likewise demonstrates an overestimation. It is a well- known fact that EN formula tends to overestimate pile capacity which can be attributed to the different values of constant "C". These constants were derived by Wellington [23] which is dependent on the extra initial resistance to get the pile in motion again and these values vary based on hammer type. Hence, from the measured capacity (Q_{L2}), the "C" constants for drop, air/steam, and diesel hammers for driven piles were back-calculated as shown in Table 13. The back-calculated C values for drop, air/steam and diesel are 40.0, 30.5, and 43.1, respectively. Obviously, these "C" values are larger than the ones previously developed, however, these may possibly provide better capacity prediction. But it is recommended to utilize more data for verification.

Table 12 Range of driving records for different hammers

Hammer type	Statistics	Rated energy (kN-m)	Final set (blows/25mm)
drop	n	7	7
	Range	2.5 -69.0	2 - 25
	Mean	14.1	11
	COV	1.72	0.72
air/steam	n	11	11
	Range	122.0 - 122.0	1 - 13
	Mean	122	5
	COV	-	0.99
Diesel	n	5	5
	Range	33.6 – 62.4	2 - 8
	Mean	48.0	5
	COV	0.26	0.45

Table 13 Statistics of QENR/QL2 and back-calculated C

Hammer type	Statistics	Q_{ENR}/Q_{L2}	Back-Calculated C
drop	n	7	7
	Mean	1.5	40.0
	SD	0.72	21.0
	COV	0.48	0.53
air/steam	n	11	11
	Mean	3.2	30.5
	SD	1.54	12.78
	COV	0.48	0.42
diesel	n	5	5
	Mean	5.4	43.1
	SD	2.06	19.16
	COV	0.38	0.44

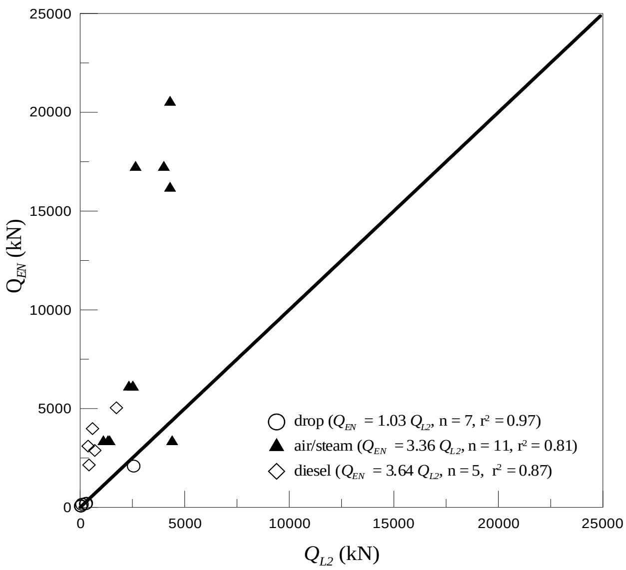

Fig. 6 Comparison of predicted (QEN) and measured (QL2) capacity of pile hammers for drained loading

8. Comparison of Driven PC Piles and Drilled Shafts

The load-displacement behavior of driven PC piles and drilled shaft are compared in order to examine more general behavior of foundation. The combined round and square data for drained and undrained were used since comparable behavior are observed for both sections and the data are consistent. Results from previous study [16] of drilled shaft is used for comparison. Figs. 7(a) and 7(b) for drained and undrained loading, respectively present the normalized load-displacement curves. For the purpose of comparison, the interpreted capacities are normalized by Q_{CHIN}. For ease in comparison, L_1 and L_2

are marked in Fig. 7(a) and 7(b). For drained loading, Fig. 7(a) demonstrates that driven pile develops somewhat larger displacement. The drilled shaft study indicated δ_{L2} = 10.6 mm while the present study has an average δ_{L2} = 18.0 mm. This behavior can be attributed to the better adhesion between the soil and shaft interface of drilled shafts that limits relatively large uplift displacement. For undrained loading in Fig. 7(b), similar phenomenon is observed wherein stiffer response is exhibited by the load-displacement curve of drilled shafts. The drilled shaft study indicated δ_{L2} = 12.1 mm for undrained loading while the present study has an average δ_{L2} = 12.5 mm.

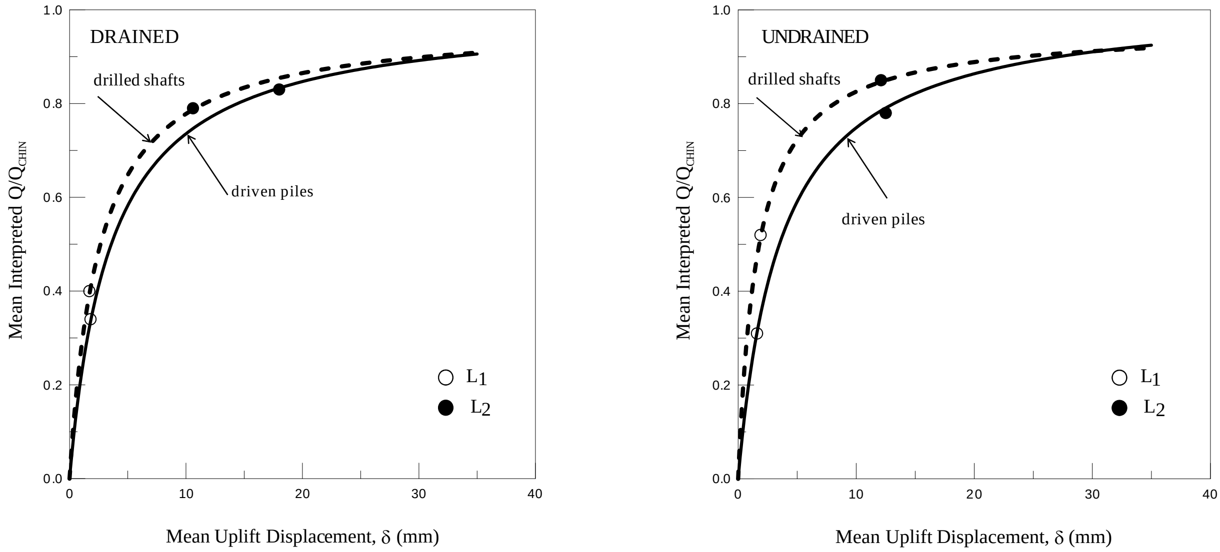

(a) drained (b) undrained

Fig. 7 Mean load-displacement comparison of driven piles and drilled shafts for uplift loading

9. Conclusions

Seven representative interpretation criteria (van der Veen, Chin, Fuller and Hoy, DeBeer, Davisson, Slope Tangent, and L_1-L_2) were evaluated based on a compiled database of driven PC piles. Axial uplift static load tests on round and square cross-section piles in various soil profiles were used for this purpose. Based on the research results for driven PC piles, the following conclusions are reached, and design recommendations are proposed for their use. DeBeer method is the lower bound criterion and considered as significant underpredictor while Chin represents the upper bound criterion and is a significant overpredictor. L_1 can be defined as the elastic limit, while L_2 can be deemed useful definition of interpreted failure load in driven piles. Fuller and Hoy, and Van der Veen can be compared to L_2. Davisson and slope tangent are modest underpredictors of L_2 but these methods are simple and convenient to use. The normalized load-displacement curves of drained round and square piles are comparable whereas for undrained loading, round pile has more ductile normalized load-displacement behavior than square piles. Capacity approximations are developed using L_1 and L_2 for both drained and undrained loading. Where needed, these ratios can be utilized to interrelate the methods such as when limited load-displacement data are available or for tests that are stopped at an early stage. Statistical analyses show that higher COV values are at smaller pile displacements, and drained loading exhibits minimal variations than undrained loading. Behavior difference between the two pile cross-sections for both drained and undrained conditions can be attributed to several factors including frictional resistance that develops on square pile surroundings, the effect of set-up, and other issues, including databases differences. Dependence of general load-displacement behavior on hammer types for both drained and undrained loading is minimal. However, great overestimation is shown by the EN formula for uplift pile capacity. Drilled shaft for both drained and undrained loading shows stiffer load-displacement response than driven piles which means that relatively larger displacements are needed to fully mobilize the capacity of driven piles. Finally, due to the limited case histories for undrained loading as compared to drained loading, more data will be included to the database in the future to provide better comparison of the seven interpretation methods that warrants significant recommendations on the applicability of each method in driven PC pile uplift capacity. Further, other important factors, such as effects of pore water pressure, pile set-up, and hammer types on pile uplift capacity should be given due consideration for future study.

Acknowledgement

This study was supported by the Center for Research and Development, Adamson University and Ministry of Science and Technology, Taiwan, under Contract No. MOST 106-2221-E-033-018.

Nomenclature

ENGLISH LETTERS - UPPER CASE

B	-	pile diameter
COV	-	coefficient of variation
D	-	pile depth
D_r	-	relative density
DUR	-	drained uplift round
DUS	-	drained uplift square
GWT	-	ground water table
L_1	-	elastic limit
L_2	-	failure threshold
P	-	load
P_{ult}	-	ultimate load
Q	-	compression capacity
Q_{CHIN}	-	interpreted capacity by Chin method
Q_{DAV}	-	interpreted capacity by Davisson method
Q_{DB}	-	interpreted capacity by DeBeer method
$Q_{F\&H}$	-	interpreted capacity by Fuller and Hoy method
Q_{L1}	-	interpreted capacity by L_1 method
Q_{L2}	-	interpreted capacity by L_2 method
Q_{ST}	-	interpreted capacity by slope tangent method
Q_{VDV}	-	interpreted capacity by Van der Veen method
SD	-	standard deviation
UUR	-	undrained uplift round
UUS	-	undrained uplift square
VST	-	vane shear test
W_r	-	hammer weight

ENGLISH LETTERS - LOWER CASE

n	-	number of data points; modulus parameter
r^2	-	coefficient of determination
s_u	-	undrained shear strength

GREEK LETTERS

δ_{CHIN}	-	displacement corresponding to Q_{CHIN}
δ_{DAV}	-	displacement corresponding to Q_{DAV}
δ_{DB}	-	displacement corresponding to Q_{DB}
$\delta_{F\&H}$	-	displacement corresponding to $Q_{F\&H}$
δ_{L1}	-	displacement corresponding to Q_{L1}
δ_{L2}	-	displacement corresponding to Q_{L2}
δ_{ST}	-	displacement corresponding to Q_{ST}
δ_{VDV}	-	displacement corresponding to Q_{VDV}

References

[1] M. Teguh, "Structural behaviour of precast concrete frames on a non-engineered building subjected to lateral loads," International Journal of Engineerng and Technology Innovation, vol. 6, no. 2, pp. 152-164, 2016.

[2] F. K. Chin, "Estimation of the ultimate load of piles from tests not carried to failure," Proc. 2nd Southeast Asian Conference on Soil Engineering, Singapore, 1970, pp. 81-92.

[3] K. Terzaghi and R. B. Peck, Soil mechanics in engineering practice, 2nd ed., John Wiley & Sons, 1967.

[4] C. Van der Veen, "The bearing capacity of a pile," Proc. 3rd International Conference on Soil Mechanics and Foundation Engineering, Zurich, 1953, pp. 84-90.

[5] E. De Beer, "Experimental determination of the shape factors and the bearing capacity factors of sand," Geotechnique, vol. 20, no. 4, pp. 387-411, 1970.

[6] F. M. Fuller and H. E. Hoy, "Pile load tests including quick-load test method, conventional methods and interpretations," Highway Research Record, http://onlinepubs.trb.org/Onlinepubs/hrr/1970/333/333-008.pdf.

[7] M. Davisson, "High capacity piles," Proc. Soil Mechanics Lecture Series on Innovations in Foundation Construction, 1972, pp. 81-112.

[8] A. Hirany and F. H. Kulhawy, "Conduct and interpretation of load tests on drilled shaft foundations: Volume 1, Detailed guidelines," Electric Power Research Institute, Palo Alto, CA (USA), 1988.

[9] A. Hirany and F. H. Kulhawy, "On the interpretation of drilled foundation load test results," Deep Foundations 2002: An International Perspective on Theory, Design, Construction, and Performance, 2002, pp. 1018-1028.

[10] B. H. Fellenius, "Test loading of piles-methods, interpretation and new proof testing procedure," Journal of the Geotechnical and Engineering Division, vol. 101, pp. 855-869, 1975.

[11] R. Duzceer and A. Saglamer, "Evaluation of pile load test results," Proc. 9th International Conference on Piling and Deep Foundation, Nice, 2002.

[12] M. C. M. Marcos, Y. J. Chen, and F. H. Kulhawy, "Evaluation of compression load test interpretation criteria for driven precast concrete pile capacity," KSCE Journal of Civil Engineering, vol. 17, no. 5, pp. 1008-1022, 2013.

[13] K. C. Birid, "Evaluation of ultimate pile compression capacity from static pile load test results," Proc. International Congress and Exhibition, Sustainable Civil Infrastructures: Innovative Infrastructure Geotechnology, Springer, 2017, pp. 1-14.

[14] Y. J. Chen and Y. C. Fang, "Critical evaluation of compression interpretation criteria for drilled shafts," Journal of Geotechnical and Geoenvironmental Engineering, vol. 135, no. 8, pp. 1056-1069, 2009.

[15] A. Hirany and F. H. Kulhawy, "Interpretation of load tests on drilled shafts-Part 2: Axial uplift," Proc. Foundation Engineering: Current Principles and Practices, ASCE, 1989, pp. 1150-1159..

[16] Y. J. Chen, H. W. Chang, and F. H. Kulhawy, "Evaluation of uplift interpretation criteria for drilled shaft capacity," Journal of Geotechnical and Geoenvironmental Engineering, vol. 134, pp. 1459-1468, 2008.

[17] Y. J. Chen and T. H. Chu, "Evaluation of uplift interpretation criteria for drilled shafts in gravelly soils," Canadian Geotechnical Journal, vol. 49, no. 1, pp. 70-77, 2011.

[18] M. Hussein and J. Sheahan, "Uplift capacity of driven piles from static loading test," Proc. of the 3rd International Conference on Case Histories in Geotechnical Engineering, St. Louis, Missouri, 1993.

[19] Z. z. Qian, X. L. Lu, X. Han, and R. M. Tong, "Interpretation of uplift load tests on belled piers in Gobi gravel," Canadian Geotechnical Journal, vol. 52, no. 7, pp. 992-998, 2015.

[20] X. L. Lu, Z. Z. Qian, and W. Z. Yang, "Axial uplift behavior of belled piers in sloping ground," Geotechnical Testing Journal, vol. 40, no. 4, pp. 579-590, 2017.

[21] T. O'rourke and F. H. Kulhawy, "Observations on load tests for drilled shafts," Proc. Drilled Piers and Caissons II,ASCE, New York, 1985, pp. 113-128.

[22] J. R. Chen, "Axial behavior of drilled shafts in gravelly soils," Ph.D dissertation, Cornell University, 2004.

[23] A. M. Wellington, Piles and pile-driving, Rarebooksclub Com, 2012.